Neurol Ther (2023) 12:2101–2119
https://doi.org/10.1007/s40120-023-00547-9

ORIGINAL RESEARCH

# Identification of miRNAs Involved in Intracranial Aneurysm Rupture in Cigarette-Smoking Patients

Hanbin Wang · Luxuan Wang · Yanli Tan · Chuan Fang · Chunhui Li · Lijian Zhang

Received: August 14, 2023 / Accepted: September 13, 2023 / Published online: October 4, 2023


## ABSTRACT

***Introduction***: Smoking is an independent risk factor for the formation and rupture of intracranial aneurysms (IA). However, the underlying mechanism remains unclear.
***Methods***: In this study, we performed miRNA sequencing on plasma from 10 smoking patients with IA, 10 non-smoking patients with IA, and 10 healthy controls. The differentially expressed miRNAs (DE miRNAs) between smoking and non-smoking patients with IA were identified. Functional and pathway enrichment analysis is employed to investigate the potential functions of those DE miRNA target genes. The correlations with the clinical parameters were assessed using receiver operating characteristic curve (ROC) analysis.
***Results***: In total, we identified 428 DE miRNAs. Functional enrichment analysis showed the target genes were significantly enriched in biological aspects related to cell characteristics, such as cell cycle, cell differentiation, and cell migration. Pathway analysis showed DE miRNAs mainly enriched in the PI3K-Akt signaling pathway, Focal adhesion, and JAK-STAT signaling pathway. The expressions of miR-574-5p, miR-151a-3p, and miR-652-3p correlated well with aneurysm parameters. The AUC of miR-574-5p, miR-151a-3p, and miR-652-3p were 97%, 92%, and 99%, respectively.
***Conclusion***: Our study indicated that smoking significantly altered the plasma miRNA profile in

Hanbin Wang and Luxuan Wang have contributed equally to this work.

**Supplementary Information** The online version contains supplementary material available at https://doi.org/10.1007/s40120-023-00547-9.

H. Wang · C. Fang (✉) · C. Li (✉) · L. Zhang (✉)
Department of Neurosurgery, Affiliated Hospital of Hebei University, Hebei University, Baoding 071000, Hebei, China
e-mail: chuanfang@hbu.edu.cn

C. Li
e-mail: lichunhui0860312@sina.com

L. Zhang
e-mail: lijian.zhang@aliyun.com

L. Wang
Department of Neurological Function Examination, Affiliated Hospital of Hebei University, Hebei University, Baoding 071000, Hebei, China

Y. Tan
Department of Pathology, Affiliated Hospital of Hebei University, Hebei University, Baoding 071000, Hebei, China

C. Fang · L. Zhang
Postdoctoral Research Station of Neurosurgery, Affiliated Hospital of Hebei University, Hebei University, Baoding 071000, Hebei, China

C. Fang
Hebei Key Laboratory of Precise Diagnosis and Treatment of Glioma, Baoding, China

patients with IA. The expression of miR-574-5p, miR-151a-3p, and miR-652-3p correlated with aneurysm parameters, which may play a significant role in the formation and rupture of IA.

**Keywords:** Intracranial aneurysm; Smoking; miRNAs; Plasma; Biomarkers

**Key Summary Points**

**Why carry out this study?**

· Smoking is an independent risk factor for the formation and rupture of intracranial aneurysms (IA). However, the underlying mechanism remains unclear.

· We performed miRNA sequencing on plasma from 10 smoking IA, 10 non-smoking IA patients, and 10 healthy controls.

We also performed functional and pathway enrichment analysis of the differentially expressed miRNA target genes. Correlations with the clinal parameters were also performed by using receiver operating characteristic curve (ROC) analysis.

**What was learned from the study?**

· Smoking could significantly alter the plasma miRNA profile in intracranial aneurysm patients.

· The expression of miR-574-5p, miR-151a-3p, and miR-652-3p correlated with aneurysm height and width.

· miR-574-5p, miR-151a-3p, and miR-652-3p showed high sensitivity and specificity for the diagnosis of intracranial aneurysm.

## INTRODUCTION

An intracranial aneurysm (IA) is an abnormal bulge in the intracranial artery wall, and its rupture can lead to subarachnoid hemorrhage, which seriously endangers patients' health [1]. The worldwide incidence of patients with IA is 3.2%, and the fatality rate and disability rate of the first rupture and hemorrhage are as high as 33% [2]. Therefore, an in-depth exploration of the mechanism of IA is particularly crucial to prevent IA formation and reduce the risk of aneurysm rupture.

So far, although the etiology of IA is unknown, smoking has been demonstrated to be an independent risk factor for IA formation and rupture, and smoking is significantly associated with IA growth and rupture [3]. Data show that the smoking history of risk of IA is four times the size of the non-smokers. The current smokers had a 2.5-fold higher risk of rupture than non-smoking patients with IA [4]. Moreover, previous studies have demonstrated that smoking could induce the formation and rupture of IA through hemodynamics, chronic inflammation, endothelial dysfunction, and vascular remodeling [4]. In our previous work, we performed a meta-analysis that showed smoking significantly increased the risk of aneurysm rupture [5]. However, the underlying mechanisms of smoking-induced IA formation and rupture are vague and require further investigation. Therefore, an in-depth exploration of its molecular mechanisms could help us to identify novel therapeutic targets or potential biomarkers, especially for smokers.

Studies have found that dysregulated microRNA (miRNA) plays important pathogenic roles in the formation and rupture of IA [6]. miRNA is a kind of endogenous single-stranded small molecule RNA with a length of about 20–24 nucleotides, which plays a huge role in cell differentiation, apoptosis, biological development, and the occurrence and development of diseases [7]. miRNAs can regulate intracellular protein synthesis and target gene expression, complex biological signaling pathways, and regulatory networks. Abnormal up- or down-regulation of miRNA may lead to cell damage and some aspects of physiological dysfunction, leading to the occurrence and development of diseases. In addition, miRNA secreted by various cells can exist stably in body fluids (serum, plasma, cerebrospinal fluid, etc.), which means miRNAs have the ability to be a potential biomarker for the diagnosis and prognosis of

various diseases [8]. Previous studies have shown that miRNAs can serve as potential molecular biomarkers for predicting IA [9]. Some studies conducted genome-wide miRNA sequencing of IA tissues and screened out miRNAs closely related to IA as potential biomarkers [10, 11]. For example, miR-331-3p is related to the phenotypic changes of vascular smooth muscle cells, which can be used as a potential marker of IA [12], and miR-29 can regulate inflammatory responses and is highly expressed in IA patients [13]. The peripheral blood, in comparison to IA tissue, offers easy accessibility, minimal trauma, and suitable dynamic detection capabilities, making it a significant source of biomarkers.

In this experiment, we employed miRNA sequencing to investigate the biological effect and potential molecular mechanism of smoking in IA formation, and to identify novel peripherally accessible biomarkers and potential therapeutic targets.

# METHODS

### Recruitment of Study Subjects and Clinical Data Acquisition

The experiment consisted of three groups: smoking IA group ($n = 10$), non-smoking IA group ($n = 10$), and healthy non-smoking control group ($n = 10$). The IA patient was diagnosed with computed tomography angiography (CTA) or digital subtraction angiography (DSA). Patients with severe systemic dysfunction or combined with other serious diseases or trauma/infectious IA were excluded. The control group consisted of age-and sex-matched non-smoking healthy volunteers. healthy volunteers with previous IA and healthy volunteers with relatives with IA were excluded from the control group.

The clinical parameters were collected, including age, sex, smoking history, smoking frequency, history of hypertension, family history of aneurysm, and rupture of the aneurysm. We used the smoking index (smoking index = the number of cigarettes smoked per day × number of years of smoking) to measure cigarette intake [14]. Smoking index categories were non-smoking, < 400, 400–799, and ≥ 800. Aneurysm parameters include aneurysm location, aneurysm size, aneurysm height, aneurysm width, and aspect ratio (aneurysm height/aneurysm width). Aneurysm height was measured as the maximum perpendicular distance between the dome and the neck plane. This study was conducted in accordance with the Declaration of Helsinki, Good Clinical Practice, and the Council for International Organizations of Medical Sciences' International Ethical Guidelines for health-related Research Involving Humans. The protocol was approved by the Medical Ethics Committee of the Affiliated Hospital of Hebei University (HDFYLL-K-Y-2022-014).

### Blood Sample Collection

The patient's blood samples were obtained within 12 h of hospitalization or before emergency surgical treatment. Venous blood samples of 10 ml from IA patients and healthy volunteers were collected and placed in EDTA tubes and stored at 4 °C for further processing within 4 h. Venous blood was centrifuged at 1600*g* for 10 min at 4 °C, and then plasma was extracted. The plasma was stored in a refrigerator at − 80 °C until further analysis.

### miRNA Isolation and Quality Control

Total RNA in plasma was extracted using the Qiagen 217004 miRNeasy Mini Kit (Kejer, Germany) according to the manufacturer's specifications. A NanoDrop was used to measure the RNA OD value of the RNA samples to determine the purity and quality of the RNA. The A260/A280 ratio of RNA was 2.0, indicating its high purity. In general, if the A260/A280 ratio is higher than 1.8, it indicates that the purity and quality of the RNA are acceptable and can be used for further experiments.

### Profiling of Plasma miRNA

The miRNA sequencing library was prepared using the TruSeq Small RNA Sample Prep Kits

(Illumina, San Diego, CA, USA) kit. After the library was prepared, the constructed library was sequenced by Illumina Hiseq2000/2500, and the sequencing read length was $1 \times 50$ bp. Clean reads were obtained after quality control processing of the original data. Then, the remaining sequences were compared with various RNA database sequences (excluding miRNA), such as the mRNA database, RFam database (including rRNA, tRNA, snRNA, snoRNA, etc.), and Repbase database (repeat sequence database), and filtered. Finally, valid data were obtained and used for subsequent miRNA data analysis.

### Bioinformatics Analysis

We used the comprehensive miRNA target gene database TargetScan (https://www.targetscan.org/) and Miranda to predict the potential target genes regulated by DE miRNA, with KEGG pathway enrichment analysis on potential target genes regulated by miRNA with DIANA-mir Path (http://www.microrna.gr/miRPathv3). In addition, we also used the plug-in bingo in Cytoscape software to perform Gene Ontology (GO) enrichment analysis on potential target genes regulated by miRNA. Enrichment analysis results with a $p$ value $< 0.05$ were considered statistically significant. Finally, a principal component analysis (PCA) model was visualized for clustering trends, based on the variation in the phase of injury using the 'principal' function in the R software.

### Statistical Analysis

Statistical analysis was performed using Graph Pad Prism v.6.0 (Graph Pad Software, CA, USA) One-way ANOVA was used to test the significant difference between miRNAs among groups. The Shapiro–Wilk test was used to evaluate the normality of the data. Pearson correlation analysis was used to assess the correlation between DE miRNAs and aneurysm parameters. The receiver operating characteristic curve (ROC) was constructed to assess the potential diagnostic efficacy of each candidate miRNA by the area under ROC (AUC). $p < 0.05$ was considered statistically significant.

## RESULTS

### General Information of Participants

A total of 30 participants were enrolled in this study, including 10 smoking IA patients, 10 non-smoking IA patients, and 10 healthy volunteers matched for age and sex (Table 1). There were 3 females and 7 males in the smoking IA group, and the mean age of the patients was $60.10 \pm 11.51$. There were 6 females and 4 males in the non-smoking IA group, and the mean age of the patients was $55.90 \pm 11.97$. In the healthy control group, there were 5 females and 5 males, and the average age of patients was $58.40 \pm 6.85$. The age distribution of the smoking ($p = 0.307$), non-smoking ($p = 0.323$), and healthy control groups ($p = 0.394$) was normal. In terms of age and sex ratio, there was no statistically significant difference between the smoking IA group, the non-smoking IA group, and the control group.

### miRNAs Profiles in Smoking IA Patients

PCA was performed to investigate the variance in these data (Fig. 1). The results showed clearly separate groups in the comparison between the IA patients and the healthy controls, the non-smoking IA group, and smoking IA group. Hierarchical cluster analysis showed that the two-way clustering of miRNAs distinctly demarcated between those three groups (Fig. 2).

Compared with the control group, 717 miRNAs were differentially expressed, with a twofold difference between the smoking IA group. Among them, 101 miRNAs were up-regulated and 616 miRNAs were down-regulated (Supplementary Table 1). Compared with the non-smoking IA group, 428 miRNAs were differentially expressed, with a twofold difference between the smoking IA group. Among them, 49 miRNAs were up-regulated and 379 miRNAs were down-regulated (Supplementary Table 2). Compared with the control group, 932 miRNAs

**Table 1** General characteristics of smoking IA patients, non-smoking IA patients, and healthy controls

| Parameters | Smoking IA ($n = 10$) | non-smoking IA ($n = 10$) | healthy controls ($n = 10$) |
|---|---|---|---|
| Age, years | 60.10 ± 11.51 | 55.90 ± 11.97 | 58.40 ± 6.85 |
| Sex, male/female | 7/3 | 4/6 | 5/5 |
| Smoking index | | | |
| non-smoking | 0 | 10 | 10 |
| < 400 | 1 | – | – |
| 400–799 | 7 | – | – |
| ≥ 800 | 2 | – | – |
| Hypertension | 6 | 7 | 7 |
| Aneurysm rupture | 10 | 10 | – |
| Aneurysm size | | | |
| < 5 mm | 3 | 5 | – |
| 5–10 mm | 5 | 4 | – |
| > 10 mm | 2 | 1 | – |
| Aneurysm height (mm) | 6.40 ± 2.88 | 5.35 ± 2.56 | – |
| Aneurysm width (mm) | 3.36 ± 1.60 | 3.69 ± 1.63 | – |

were differentially expressed, with a twofold difference between the non-smoking IA group. Among them, 320 miRNAs were up-regulated and 612 miRNAs were down-regulated (Supplementary Table 3).

## Target Gene Prediction of Differential miRNAs

To elucidate the biological function of these differentially expressed miRNAs (DE miRNAs), we used the online tool TargetScan and Miranda to predict their target genes. The DE miRNAs between the smoking and non-smoking groups had 17,499 target genes. The DE miRNAs between the smoking and healthy control groups had 15,329 target genes. The DE miRNAs between the non-smoking and healthy control groups had 13,095 target genes (Supplementary Table 4).

## Enrichment Pathway and Gene Ontology Analysis

To determine the functional annotation of validated target genes of the DE miRNAs between the smoking IA and nonsmoking IA groups, we performed GO enrichment assays to assess the biological significance of differently expressed miRNAs. GO is a widely used ontology in the field of bioinformatics, which covers three aspects of biology: cell composition (CC), molecular function (MF), and biological process (BP). Figure 3a–c shows the most remarkable association terms for each ontology in the GO enrichment analysis. We found that the target gene of the DE miRNAs between the smoking IA and non-smoking IA groups were involved in many biologically essential cell compositions, molecular functions, and biological processes, including cytoplasm, nucleus, nucleoplasm, cytoplasmic vesicle, etc. Detailed results of the

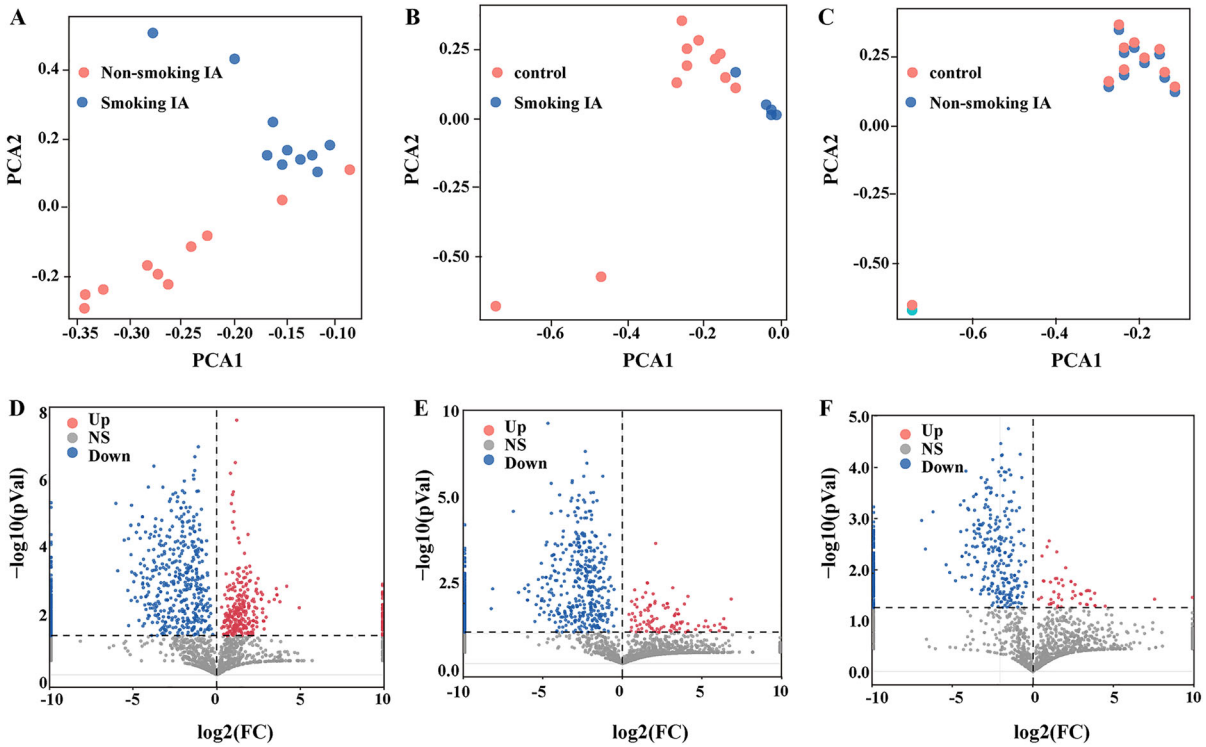


**Fig. 1** Identification of differentially expression miRNA in the smoking IA and non-smoking IA patients. **A** The variance in miRNAs expression between smoking IA patients and non-smoking IA patients. **B** The variance in miRNAs expression between healthy control and smoking IA patients. **C** The variance in miRNAs expression between healthy control and non-smoking IA patients. **D** Volcano map of DE miRNA between smoking IA patients and non-smoking IA patients. **E** Volcano map of DE miRNA between healthy control and smoking IA patients. **F** Volcano map of DE miRNA between healthy control and non-smoking IA patients. *X*-axis: log2FC; *Y*-axis: $-\log_{10}$ (PVal). Blue down-regulated miRNAs, red up-regulated miRNAs, grey non-significant

GO enrichment analysis are shown in Table 2. Pathway analysis of DE miRNAs between the smoking IA and non-smoking IA groups showed that they were highly enriched in multiple signaling pathways. As Fig. 3d shows, the top 20 KEGG pathways included pathways in cancer, the PI3K-Akt signaling pathway, etc. Detailed results of the KEGG enrichment analysis are shown in Table 2. Figure 4a shows the target gene enrichment analysis results of DE miRNAs between the smoking IA and the healthy control groups. We found that the target genes of DE miRNAs were involved in many essential processes and pathways, such as protein binding, metal ion binding, DNA binding, etc. Figure 4b shows the target gene enrichment analysis results of DE miRNAs between the non-smoking IA and the healthy control groups. We found that the target genes of DE miRNAs were also involved in many essential processes and pathways, such as protein binding, DNA binding, transcriptional regulation, etc.

## Correlation and ROC Curve Analysis

Among the DE miRNAs between the smoking IA and healthy control groups, miR-320a-3p, miR-4732-5p, miR-652-3p, miR-424-5p, miR-26a-5p, and miR-574-5p were found to be correlated with aneurysm parameters (Fig. 5), miR-320a-3p ($p < 0.045$, $r = 0.642$), miR-652-3p ($p < 0.047$, $r = 0.638$), and miR-424-5p ($p < 0.021$, $r = 0.711$) were positively correlated with aneurysm height, miR-4732-5p ($p < 0.029$, $r = 0.684$) and miR-574-5p ($p < 0.03$, $r = 0.853$)

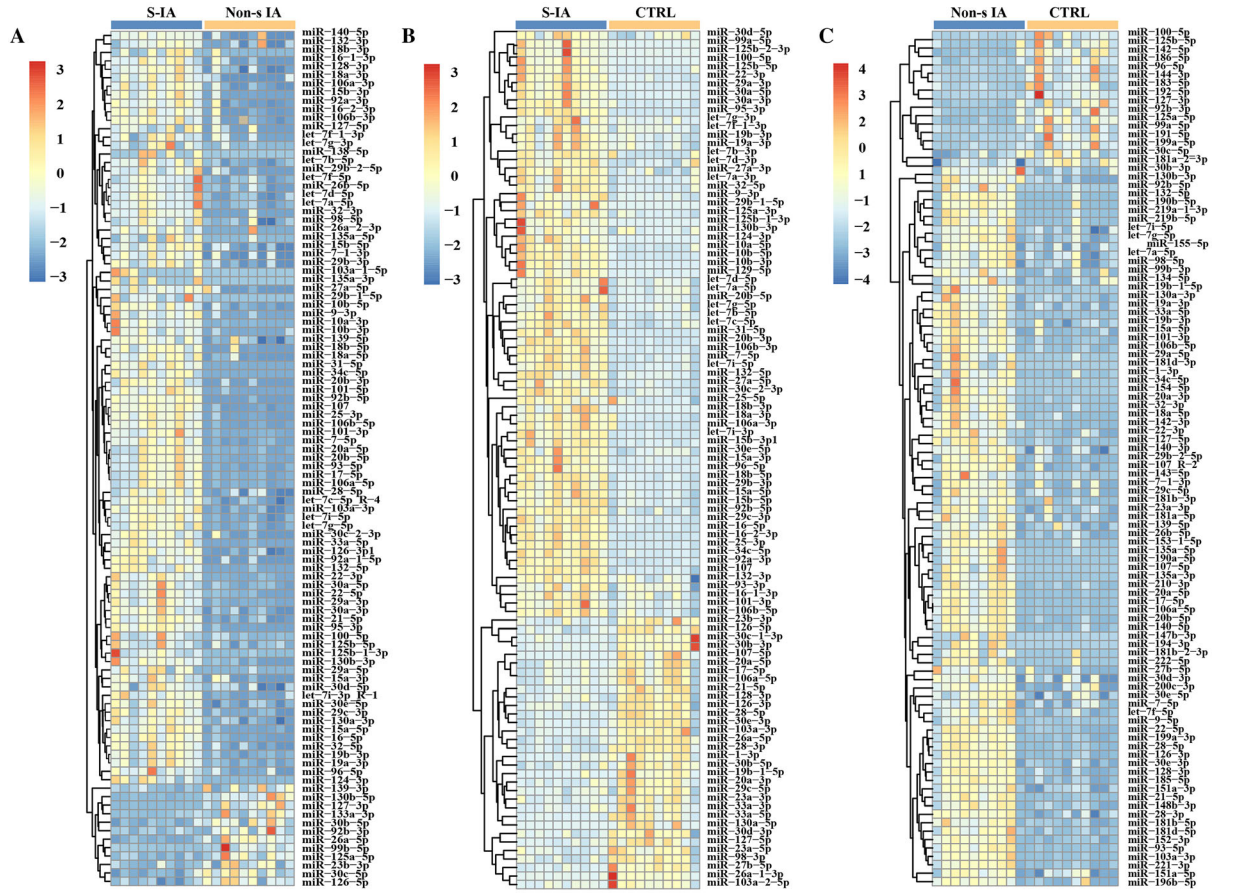


**Fig. 2** Plasma miRNA expression profiles of smoking IA patients, non-smoking IA patients, and healthy control group. **A** The heat map of DE miRNA between smoking IA and non-smoking IA. **B** The heat map of DE miRNA between smoking IA and healthy control groups. **C** The heat map of DE miRNA between non-smoking IA and healthy control groups. The horizontal axis of the heat map is the sample, and the vertical axis is the miRNA. Different colors indicate different miRNA expression levels, and the colors from blue to white to red indicates the expression level from low to high. S-IA smoking intracranial aneurysm, Non-s IA non-smoking intracranial aneurysm, CTRL control

were positively correlated with aneurysm height/width, and miR-26a-5p was negatively correlated with aneurysm width ($p < 0.042$, $r = -0.649$). Among the DE miRNAs between the smoking IA and non-smoking IA groups, miR-574-5p, miR-151a-3p, and miR-652-3p were found to be correlated with aneurysm parameters (Fig. 6a), miR-652-3p ($p < 0.047$, $r = 0.638$) was well correlated with aneurysm height, miR-151a-3p ($p < 0.048$, $r = -0.637$) was well correlated with aneurysm width, and miR-574-5p ($p < 0.03$, $r = 0.853$) was well correlated with aneurysm height/aneurysm width. The correlation analysis revealed that miR-151a-3p expression was negatively correlated with the smoking index ($p = 0.048$, $r = -0.634$). The expression levels of miR-574-5p ($p = 0.247$, $r = -0.403$) and miR-652-3p ($p = 0.315$, $r = -0.354$) were not correlated with the smoking index (Fig. 6b).

Further, the ROC analysis showed that the sensitivity and specificity of miR-574-5p are 90% and 90%, respectively, of miR-151a-3p are 100% and 80%, respectively, and of miR-652-3p are 100% and 90%, respectively. The AUC of miR-574-5p, miR-151a-3p, miR-652-3p are 97%, 92%, and 99%, respectively (Fig. 6c).

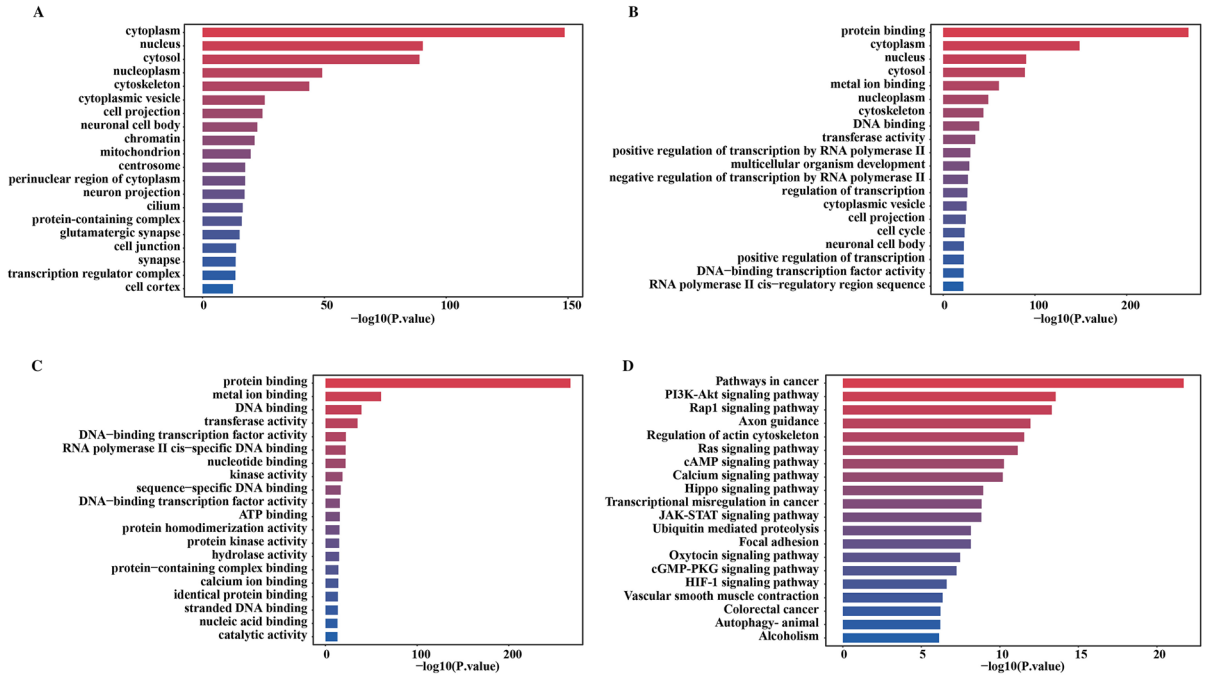


**Fig. 3** GO enrichment and KEGG pathway analysis of differentially expressed miRNAs between the smoking and non-smoking IA groups. **A** GO categories of biological processes (BP). **B** GO categories of cellular components (CC). **C** GO categories of molecular functions (MF). **D** KEGG pathway analysis of the DE miRNAs

## DISCUSSION

Previous studies have documented that smoking is one of the important independent risk factors for IA formation and rupture [5], and have demonstrated that smoking could induce the formation and rupture of IA through hemodynamics, chronic inflammation, vascular endothelial dysfunction, and vascular remodeling [15]. However, the potential molecular mechanism remains unclear and requires further study. Characterization of miRNAs profiles could provide insight into possible mechanisms that may be present during disease formation [16, 17].

In this study, we employed miRNA sequencing technology aiming to investigate the biological effect and potential molecular mechanism of smoking in IA formation. Our results showed that 428 miRNAs were differentially expressed between the smoking and non-smoking IA groups, including 49 up-regulated miRNAs and 379 down-regulated miRNAs. A total of 717 miRNAs were differentially expressed between the smoking IA and healthy controls, including 101 up-regulated and 616 down-regulated miRNAs. There were 932 miRNAs differentially expressed between the non-smoking IA and healthy controls, including 320 miRNAs up-regulated and 612 miRNAs down-regulated. We further analyzed the DE miRNA between the smoking IA and non-smoking IA groups. The results of the GO enrichment analysis showed that the DE miRNAs were significantly enriched in biology related to cell properties, especially in cell cycle, cell differentiation, cell migration, cell cycle, cell adhesion, transcriptional regulation, and protein binding. As previous studies have reported, the apoptosis and proliferation of vascular endothelial cells and vascular smooth muscle cell and infiltration of immune cells are the two principal causes of IA formation and rupture [18]. Smoking could cause these two main pathophysiological processes to induce the formation and rupture of IA [4]. In addition, the KEGG

**Table 2** GO Functional enrichment and pathway enrichment analysis of differentially expressed miRNA target genes

| GO | | | |
|---|---|---|---|
| **Term** | **Category** | ***P* value** | **UniProt ID** |
| BP | | | |
| Positive regulation of transcription by RNA polymerase II | GO:0045944 | 3.61113E−33 | DLX6, ETV1, PAX6, TFAP2B, PAX7, DCN, CALCOCO1,SLC30A9, HGF, IKZF2, |
| Regulation of transcription, DNA-templated | GO:0006355 | 1.55795E−28 | NFYA, ZFX, ZNF263, DLX6, ETV1, PAX6, TFAP2B, PAX7, ZNF207, SCMH1 |
| Multicellular organism development | GO:0007275 | 2.13391E−30 | WNT16, DLX6, IFRD1, GAS7, PAX6, SCMH1, FYN, BTBD7, SPAST, MUSK |
| Negative regulation of transcription by RNA polymerase II | GO:0000122 | 5.32813E−28 | ZNF263, PAX6, TFAP2B, STRAP, CUL3,HDAC9, NEDD4L, MXD1, MXD1, HIPK2 |
| Cell cycle | GO:0007049 | 3.95899E−26 | KMT2E, RALA, DBF4, ZNF207, TTC19, SPAST, CUL3, BOD1L1, SPDL1, CTDP1, |
| Positive regulation of transcription, DNA-templated | GO:0045944 | 3.61113E−33 | DLX6, ETV1, PAX6, TFAP2B, PAX7, DCN, CALCOCO1, SLC30A9, HGF, IKZF2 |
| Nervous system development | GO:0007399 | 2.16476E−23 | DLX6, KDM7A, GAS7, TENM1, SPAST, GPM6B, ARID1B, NEXMIF, CAMK2B, MEF2A |
| Cell differentiation | GO:0030154 | 3.59095E−21 | ABCB5, DLX6, ETV1, IFRD1, GAS7, PAX6, FYN, SPAST, GLRX2, MUSK |
| Phosphorylation | GO:0016310 | 1.52377E−20 | AK2, MAP3K14, CDKL5, FYN, MAP4K3, MUSK, EPHA3, MAPK9, PIK3CB,EIF2AK2 |
| Angiogenesis | GO:0001525 | 1.73547E−19 | NOX1, NRXN3, CALCRL, RORA, TGFBR3, CEACAM1, NRCAM, ANGPT2, NRP1, POFUT1 |
| MF | | | |
| Protein binding | GO:0005515 | 2.9008E−264 | GCLC, NFYA, NIPAL3, ANKIB1, HECW1, LASP1, M6PR,CFLAR, VPS50, ST7 |
| Metal ion binding | GO:0046872 | 1.37913E−65 | ANKIB1, LASP1, KMT2E, ITGAL, ZFX, ZNF263, KDM7A, DBF4, CACNA2D2, NOX1 |
| Transferase activity | GO:0016740 | 3.73593E−37 | ANKIB1, HS3ST1, HECW1,AK2, MAP3K14, CDKL5, UBE3C, REV3L, POMT2, FYN |
| DNA binding | GO:0003677 | 1.59763E−34 | NFYA, ZNF263, ZFY, DLX6, ETV1, PHTF2, PAX6, TFAP2B, REV3L, PAX7 |

**Table 2** continued

| GO | | | |
|---|---|---|---|
| **Term** | **Category** | ***P* value** | **UniProt ID** |
| DNA-binding transcription factor activity, RNA polymerase II-specific | GO:0000981 | 6.52672E−25 | NFYA, ZFX, DLX6, MNT, ETV1, PAX6, TFAP2B, PAX7, MXD1, FOXJ2 |
| RNA polymerase II cis-regulatory DNA binding region sequence-specific DNA binding | GO:0000978 | 1.02216E−24 | NFYA, DLX6, ETV1, PAX6, TFAP2B, CALCOCO1, MXD1, FOXJ2, NFYC, MEF2A |
| Nucleotide binding | GO:0000166 | 2.04842E−23 | ASNS, STK10, MAP2K5, CDK13, NAIP, STRADB, EIF2AK1, SLC22A4, REM1, OAS1 |
| Kinase activity | GO:0016301 | 9.56582E−20 | AK2, MAP3K14, CDKL5, FYN, MAP4K3, MUSK, EPHA3, MAPK9, PIK3CB, EIF2AK2 |
| Sequence-specific DNA binding | GO:0043565 | 3.36805E−19 | ZNF263, DLX6, ETV1, PAX6, TFAP2B, PAX7, CALCOCO1, FOXJ2, TP53BP1, CBFB |
| DNA-binding transcription factor activity | GO:0003700 | 1.97388E−18 | NFYA, ZNF263, DLX6, ETV1, PAX6, TFAP2B, PAX7, ZNF207, WIZ, IKZF2 |
| CC | | | |
| Cytoplasm | GO:0005737 | 3.5946E−152 | ANKIB1, WNT16, HECW1, LASP1, CFLAR, AK2, CDC27, KMT2E, IBTK, MAP3K14 |
| Cytosol | GO:0005829 | 5.06695E−97 | GCLC, HECW1, CFLAR, VPS50, CDC27, MAP3K14, AP2B1, FARP2, PAX6, SYN1 |
| Nucleus | GO:0005634 | 1.93966E−86 | NFYA, CDC27, KMT2E, IBTK, ZFX, ZNF263, DLX6, KDM7A, ETV1, PHTF2 |
| Cytoskeleton | GO:0005856 | 1.21282E−47 | LASP1, KMT2E, FARP2, GAS7, SYN1, CDKL5, TENM1, ZNF207, SLC30A9, SPAST |
| Nucleoplasm | GO:0005654 | 5.30388E−51 | NFYA, CDC27, KMT2E, IBTK, ZFX, MAP3K14, KDM7A, DBF4, PAX6, TFAP2B |
| Cytoplasmic vesicle | GO:0031410 | 1.81706E−27 | LAMP2, SPAG9, IYD, HFE, SLC30A9, SPAST, GABRA1, VEZT, SLC4A7, SLC18A1 |
| Cell projection | GO:0042995 | 6.32442E−27 | NOX1, CDKL5, ADAM22, EHD3, CD44, VEZT, SNX1, IFT88, SLC4A7, CUL3 |
| Neuronal cell body | GO:0043025 | 4.53325E−22 | TAC1, GLRX2, CASR, USH2A, LRP6, CDC42, TRPC5, FBXW11, MAP2, CHRNA3 |
| Mitochondrion | GO:0005739 | 1.13123E−20 | GCLC, AK2, ABCC8, FYN, TTC19, LARS2, GLRX2, ADSS2, TRIT1, HSPA5 |
| Centrosome | GO:0005813 | 1.85671E−20 | CDC27, CDKL5, TTC19, SPAST, RRAGD, IFT88, LRRC7, CUL3, BOD1L1, OFD1 |

**Table 2** continued

| GO | | | |
|---|---|---|---|
| **Term** | **Category** | ***P* value** | **UniProt ID** |
| KEGG | | | |
| PI3K-Akt signaling pathway | hsa04151 | 4.41E−16 | KITLG, PIK3CB, PPP2R5A, GNB5, PPP2R3A, ITGA8, COL4A4, ANGPT2, JAK2, MAPK1, FLT1, SGK3, IL7, CDK6,RPS6KB1,NFKB1, CDKN1B, LAMA4, GHR, PRLR |
| Focal adhesion | hsa04510 | 1.49265E−09 | PPP1CB, FYN, HGF, BIRC3, VCL, MAPK9, PIK3CB, MYLK, ROCK1, CDC42, ACTN1, PAK3, ITGA8, COL4A4, MAPK1, FLT1, CAV2, MAPK8, MAPK10, BIRC2 |
| Calcium signaling pathway | hsa04020 | 7.41132E−11 | PHKA2, PTGER3, CAMK2B, ATP2B4, MYLK, PHKA1, ATP2B1, P2RX7, SLC8A3, PHKB, STIM2, ADRA1A, ADCY7, PTGFR, ITPR2, PLCG1, CHRM3, LHCGR, PLCE1, PPP3CA |
| JAK-STAT signaling pathway | hsa04630 | 2.08628E−09 | IFNGR1, PIK3CB, PIAS2, JAK2, IL7, GHR, IL12B, PRLR, LIFR, STAM2, AKT3, PIK3CA, IL13RA1, RAF1, STAM, IFNA21, EGF, EGFR, IFNAR2, JAK1 |
| Pathways in cancer | hsa05200 | 1.20E−23 | WNT16, RALA, HGF, BIRC3, FAS, IFNGR1, KITLG, PTGER3, MAPK9, PIK3CB, CAMK2B, ROCK1, GNB5, LRP6,DC42, WNT8B, PLD1, MLH1, ARAF, RUNX1T1 |
| Rap1 signaling pathway | hsa04015 | 5.98534E−14 | ITGAL, RALA, FARP2, HGF, KITLG, PIK3CB, CDC42, GNAO1, ANGPT2, MAPK1, FLT1, MAPK14,PRKD3, RAP1A, AKT3, CNR1, FGF23, ADCY7, PIK3CA, PLCG1, |
| Axon guidance | hsa04360 | 2.09295E−13 | CRKL, FYN, EPHA3,PIK3CB, CAMK2B, ROCK1, CDC42, TRPC5, SEMA3A, PAK3, SSH1, SEMA6A, NRP1, MAPK1, FZD3, UNC5A, WNT5A, EPHA4, PIK3CA, PLCG1, |
| Ras signaling pathway | hsa04014 | 5.20834E−12 | RALA, HGF, KITLG, MAPK9, PIK3CB, GNB5, CDC42, PLD1, PAK3, BRAP, ANGPT2, MAPK1, FLT1, MAPK8, RAB5C, NFKB1, MAPK10, GAB1, RAB5B, EXOC2 |
| cAMP signaling pathway | hsa04024 | 2.06924E−10 | PTGER3, MAPK9, PIK3CB, CAMK2B, ATP2B4, PDE4A, ROCK1, ATP2B1, PLD1, ADCYAP1R1, MAPK1, MAPK8, NFKB1, MAPK10,PDE4D, RAP1A, AKT3, CREB1, GRIA2, ADCY7 |

**Table 2** continued

| GO | | | |
|---|---|---|---|
| **Term** | **Category** | ***P* value** | **UniProt ID** |
| Hippo signaling pathway | hsa04390 | 1.8018E−09 | WNT16, MPP5, FBXW11, WNT8B, DLG1, AFP, AXIN1, FZD3, TGFBR1, WNT3, BIRC2, BMP5, WNT5A, BMP2, DLG4, PATJ, CSNK1D, WNT9A, TCF7L2, PPP2R2B |

Category refers to the pathway functional categories

pathway enrichment analysis showed that the DE miRNAs were mainly involved in the PI3K-Akt signaling pathway, focal adhesion, the calcium signaling pathway, and the JAK-STAT signaling pathway. Notably, these signaling pathways are closely related to immune inflammation [19]. Inflammation is a pivotal pathophysiological process in the occurrence, development, and rupture of IA. The PI3K-Akt signaling pathway has been shown to play an important role in the formation of IA [20]. The PI3K-Akt signaling pathway also participated in abdominal and thoracic aortic aneurysms [21, 22]. Evidence has shown that the PI3K-Akt signaling pathway could also regulate tight connections in endothelial cells, leading to structural changes in the inner membrane and to immune cell infiltration [23]. Vascular inflammation and vascular injury caused by immune cell infiltration of vascular endothelium are the initial factors of aneurysm formation [18]. In addition, the PI3K/Akt pathway regulated the activation of NF-kb through IRB, which is critical for the occurrence and development of inflammation and vascular remodeling [24–26]. The JAK-STAT signaling pathway affects arterial wall inflammation and aneurysm formation. Studies have found that IL-6 could directly promote the proliferation of VSMCs and the release of monocyte chemokine-1 through the JAK/STAT signaling pathway, promoting atherosclerosis and potential aneurysm formation [27]. Studies have also found that the calcium signaling pathway regulates IκB-α and IκB-β through different molecular mechanisms, mediating the activation of NF-κB, which in turn participates in the activation of the calcium signaling pathway by regulating the expression and activation of different types of calcium channels [28]. Jayaraman et al. demonstrated activation of calcium signaling molecules and increased focal calcium concentrations in the aneurysm wall [29]. The up-regulation of calcium channels may cause damage and death of smooth muscle cells, and nicotine in cigarettes can affect calcium channels [30]. Furthermore, calcium signaling can regulate the TLR signaling pathway. NF-κB signaling and TLR signaling mediate the inflammatory response in IA [31]. Our results indicate that smoking may promote the occurrence and development of IA by affecting the above pathways. However, the functional details of these miRNA still need to be further clarified.

The morphological changes of IA could reflect the process of their occurrence, growth, and rupture potential. Previous studies have demonstrated differences in aneurysm morphology between smokers and non-smokers, and smoking may influence aneurysm morphological changes promoting the rupture of IA [32]. To further understand the effect of smoking on aneurysm morphology, we collected aneurysm parameters and analyzed their correlation with DE miRNAs expression levels. Our results showed that miR-574-5p, miR-151a-3p, and miR-652-3p in DE miRNAs correlated with aneurysm parameters. Among them, the expression levels of miR-652-3p were positively correlated with aneurysm height, miR-151a-3p was negatively associated with aneurysm width, and miR-574-5p was positively correlated with aspect ratio. Previous studies have shown that the alternation of these 3 miRNAs participated

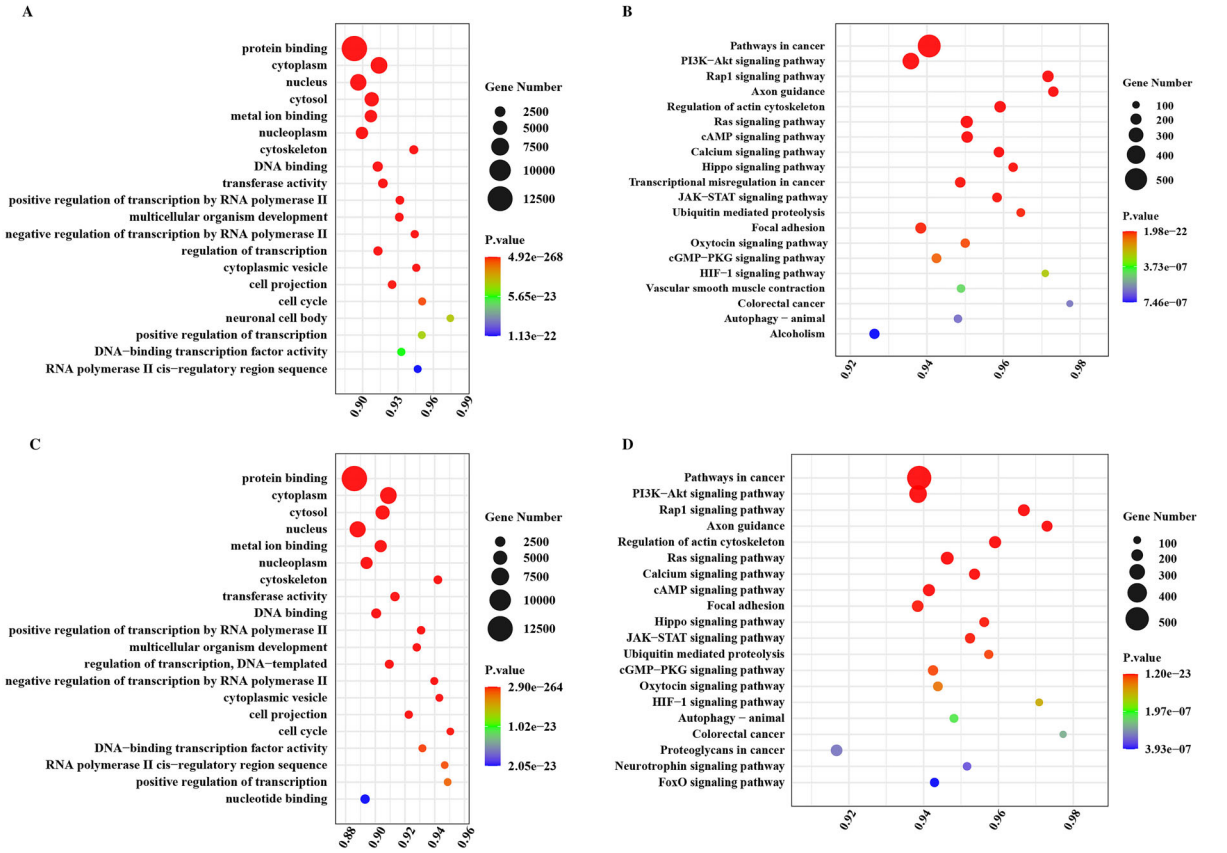


**Fig. 4** GO enrichment analysis and KEGG analysis of the DE miRNAs targeted gene between smoking IA and non-smoking IA groups. **A** GO categories of biological processes (BP). **B** GO categories of cellular components (CC). **C** GO categories of molecular functions (MF). **D** KEGG pathway analysis of the DE miRNAs targeted gene

in the pathological process of various cardiovascular diseases. The results obtained from Lai and his colleagues indicated that the overexpression of miR-574-5p could promote cell proliferation and inhibited apoptosis in VSMCs [33]. For miR-652-3p, evidence has emphasized its critical role in modulating EC proliferation and macrophage infiltration, which are important in preventing atherosclerotic progression [34]. Additionally, miR-574-5p has been shown to be correlated with the size of the aneurysm in the model of thoracic aortic aneurysm [35]. Here, our results provide evidence that smoking can affect morphological changes in IA. The relationship between smoking and these aneurysm morphological parameters may offer a morphological foundation for understanding how smoking contributes to aneurysm development and rupture. However, although the relationship between smoking and IA aneurysm parameters has been well described, the specific mechanism underlying this relationship remains unclear and is still worthy of further study.

Studies have found a dose–response relationship between smoking intensity, smoking duration, and the incidence of IA rupture [4]. As the number of cigarettes smoked per day and the duration of smoking increased, the risk of IA rupture increased accordingly. The smoking index was positively correlated with the risk of aneurysm rupture [36]. We analyzed the correlation between miR-574-5p, miR-151a-3p, and miR-652-3p and the smoking index. The results showed that the expression level of miR-151a-3p was negatively correlated with the smoking

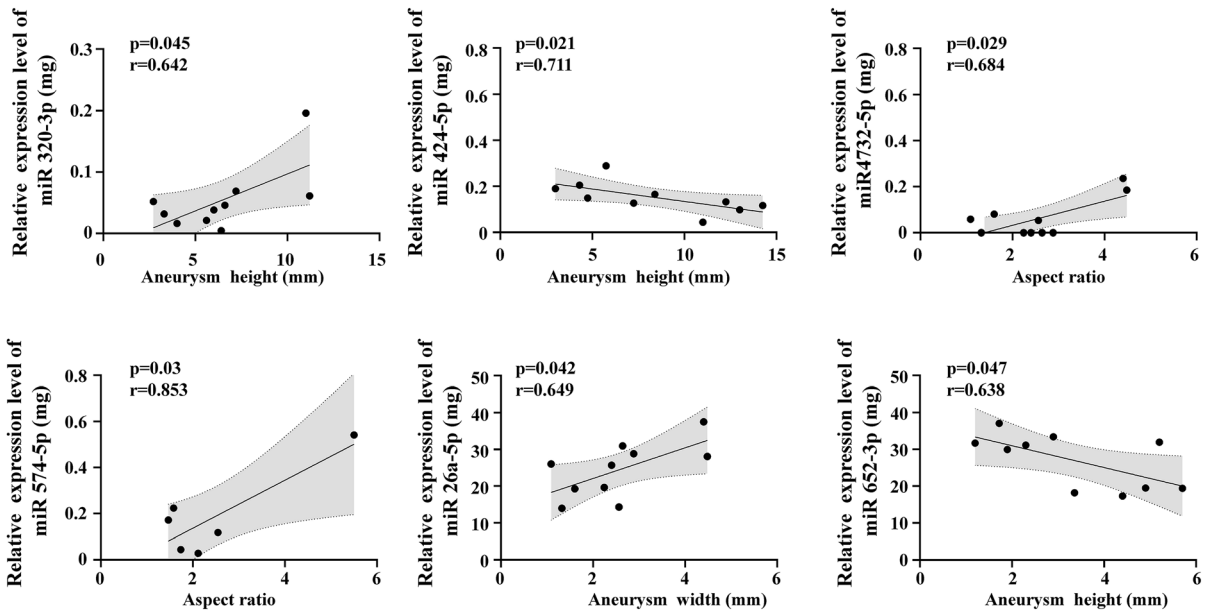


**Fig. 5** Correlation analysis and ROC analysis of miR-320a-3p, miR-4732-5p, miR-652-3p, miR-424-5p, miR-26a-5p, and miR-574-5p with aneurysm parameters

index. Combined with previous findings, we believe that the lower the plasma miR-151a-3p expression level in patients who smoke IA, the higher the smoking index, which may mean that the risk of IA rupture in smoking IA patients is also higher.

We further performed ROC analysis on miR-574-5p, miR-151a-3p, and miR-652-3p to evaluate their predictive accuracy for smoking IA. The results showed that they had good predictive efficacy against smoking IA. Among them, miR-652-3p and miR-574-5p were DE miRNAs between the smoking IA group and the non-smoking IA group, but also between the smoking IA group and the healthy control group, which may serve as potential biomarkers for IA patients with smoking. In smoking IA, miR-574-5p, miR-151a-3p, and miR-652-3p were down-regulated. Previous bioinformatics study has demonstrated that miR-574-5p participated in several biological pathways including "regulation of smooth muscle cell proliferation", "positive regulation of cellular proliferation" and "positive regulation of cell motion" [37]. Evidence has also showed that miR-574-5p is closely related to the proliferation, apoptosis, and migration of VSMCs [38]. The balance between the proliferation and apoptosis of VSMCs and the corrected alignment is critical for aneurysm growth [39]. Studies have shown that down-regulated miR-574-5p could induce the phenotype change of VSMCs from a contractile state to a secretory state, and participate in the formation of an aortic aneurysm [35]. Nakajima et al. found that phenotypic regulation of VSMCs also exists in the IA wall, and is involved in the formation and progression of IA [40]. miR-574-5p might be involved in the phenotypic regulation of VSMCs in IA. IA is a chronic inflammatory disease mediated by macrophages, and macrophage-mediated chronic inflammation plays a pivotal role in its pathogenesis [41]. Until recently, miR-151-3p could not be predicted using bioinformatics tools, even with the loosest parameters, while its function is far from clear. Previous studies showed that miR-151-3p plays an important role in maintaining the internal homeostasis of macrophages and preventing macrophages from producing inflammatory responses, while down-regulation of miR-151-3p leads to up-regulation of Stat3, which in turn promotes the production of many Stat3-dependent genes, such as the pro-inflammatory cytokine IL-6

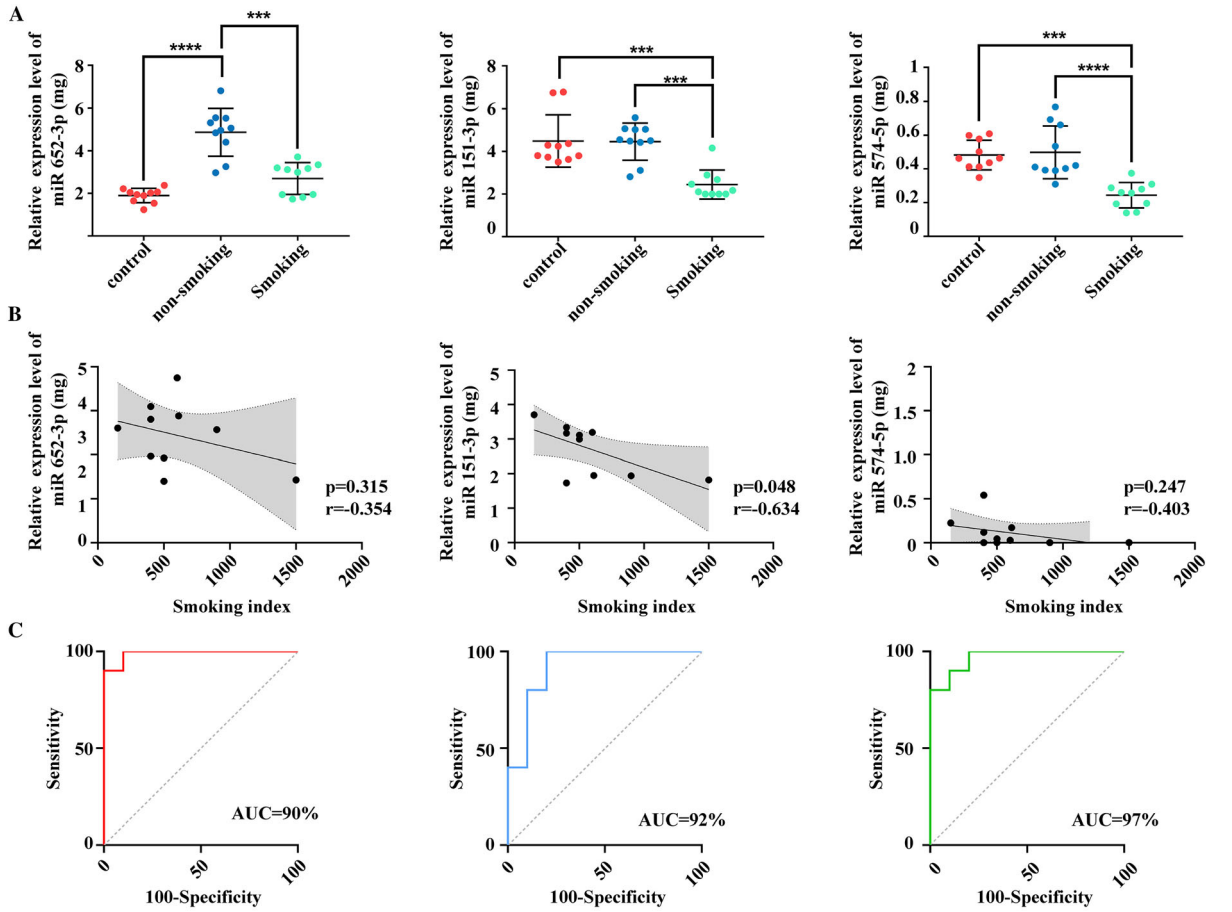


**Fig. 6** Correlation analysis and ROC analysis of miR-574-5p, miR-151a-3p, and miR-652-3p. **A** Relative expression levels of miR-652-3p, miR-151a-3p, and miR-151a-3p in non-smoking and smoking IA and healthy controls. **B** Correlation between expression levels of three plasma miRNAs and the smoking index. **C** ROC analysis of miR-574-5p, miR-151a-3p, and miR-652-3p. Data are presented as the mean ± SD. $^{**}p < 0.01$, $^{***}p < 0.0002$, $^{****}p < 0.0001$, *ns* no statistical significance

[42]. In the Stat superfamily, active Stat3 is critical in signal transduction of cytokine function and production of pro-inflammatory cytokines [43]. miR-151-3p may be involved in the inflammatory response in IA. Sugiyama et al. found atherosclerotic wall properties in the aneurysm wall of IA [44], with the presence of lipids, oxidized lipids, and apolipoprotein B-100 [45]. A single miRNA can target multiple genes to modulate a signaling network. Previous studies have reported that miR-652-3p participated in several pathological processes, including endothelial repair and the proliferation, migration, and invasion of tumor cells [46, 47]. Evidence also indicates that miR-652-3p is closely related to lipid accumulation and lipid metabolism. Recent studies have found that miR-652-3p can promote the development of atherosclerosis by regulating lipid metabolism and inflammatory cytokine secretion in macrophages [48]. There is a consistent trend between a decrease in miR-652-3p levels and an increase in the incidence of atherosclerotic lesions [49]. These studies support our findings that the down-regulation of miR-574-5p, miR-151a-3p, and miR-652-3p may play a potentially important role in the occurrence and development of IA caused by smoking and could serve as diagnostic biomarkers or therapeutic targets.

In addition, female gender and increasing age are the most widely accepted risk factors for the formation and rupture of IA [50]. Some studies have suggested that miRNA expression levels may be influenced by age and sex. For example, the expression level of miR-21 gradually increases with age, and the expression level of miR-146a is generally higher in women than in men [51]. However, as with the relationship between miR-574-5p, miR-151a-3p, and miR-652-3p and age and sex, there is no clear research result showing that there is a direct correlation between them. Moreover, there is no direct evidence of a specific relationship between miR-574-5p, miR-151a-3p, and miR-652-3p. Also, the detailed mechanism and biological roles of miR-574-5p, miR-151a-3p, and miR-652-3p in patients with IA are still unclear, which is worthy of further study.

There are some limitations to our study. First, our sample size is too small, which may affect the accuracy of our results to some extent. In the future, we need to validate the DE miRNAs in larger cohorts. Second, the small sample size also limited us from performing subgroup analyses of patients with IA who smoked according to smoking status or frequency. In addition, this study focused on the underlying molecular mechanism of smoking in patients with IA, so we did not conduct further discussion and research on the results of other intergroup experiments. Finally, the results of our study need to be validated in large-scale studies by both in vivo and in vitro methods.

## CONCLUSION

In this study we characterized the plasma miRNome of patients with IA with or without smoking. Our results showed that the smoking could result in a strong disturbance of plasma miRNA profile. We identified panels of DE miRNAs, including miR-574-5p, miR-151a-3p, and miR-652-3p, with high potential to predict aneurysm parameters which could serve as diagnostic biomarkers or therapeutic targets.

## ACKNOWLEDGEMENTS

The authors would like to thank all study participants.

***Author Contribution.*** Hanbin Wang: Investigation, Data curation, Software, Validation, Formal analysis, Investigation, Data curation, Writing-Original Draft. Luxuan Wang: Investigation, Data curation, Software, Validation, Formal analysis, Investigation, Data curation, Writing. Yanli Tan: Investigation, Data curation, Validation. Chuan Fang: Conceptualization, Review, Editing, Project administration. Chunhui Li: Conceptualization, Methodology, Validation, Formal Analysis, Review, Editing, Project administration. Lijian Zhang, PhD: Conceptualization, Investigation, Data curation, Writing, Review, Editing.

***Funding.*** This work was supported by National Natural Science Foundation of China (82201541); China Postdoctoral Science Foundation (2022M710997); Provincial Medical Talents Project funded of Hebei Province (361007); The Scientific Research Starting Foundation of Affiliated Hospital of Hebei University (31010413). The journal's Rapid Service fee was funded by the authors.

***Data Availability.*** The public sequencing data presented in the study are deposited in the GEO repository: https://www.ncbi.nlm.nih.gov/geo/query/acc.cgi?acc=GSE231922.

### *Declarations*

***Conflict of Interest.*** All named authors state no conflict of interest.

***Ethical Approval.*** All of the procedures involved in human participants in this study met the moral standards of the national research committee and the 1964 Helsinki Declaration and its subsequent amendments. This study has been approved by the Medical Ethics Committee of the Affiliated Hospital of Hebei University. (HDFYLL-K-Y-2022-014). All participants signed informed consent of this study.

## REFERENCES

1. Etminan N, Dörfler A, Steinmetz H. Unruptured intracranial aneurysms—pathogenesis and individualized management. Deutsches Arzteblatt Int. 2020;117(14):235–42.

2. Tawk RG, Hasan TF, D'Souza CE, Peel JB, Freeman WD. Diagnosis and treatment of unruptured intracranial aneurysms and aneurysmal subarachnoid hemorrhage. Mayo Clin Proc. 2021;96(7):1970–2000.

3. Jin D, Song C, Leng X, Han P. A systematic review and meta-analysis of risk factors for unruptured intracranial aneurysm growth. Int J Surg. 2019;69:68–76.

4. Can A, Castro VM, Ozdemir YH, Dagen S, Yu S, Dligach D, et al. Association of intracranial aneurysm rupture with smoking duration, intensity, and cessation. Neurology. 2017;89(13):1408–15.

5. Wang H, Wang L, Wang J, Zhang L, Li C. The biological effects of smoking on the formation and rupture of intracranial aneurysms: a systematic review and meta-analysis. Front Neurol. 2022;13:862916.

6. Feng X, Peng F, Zhang B, Wang L, Guo E, Li Y, et al. Lower miR-143/145 and higher matrix metalloproteinase-9 levels in circulation may be associated with intracranial aneurysm formation and rupture: a pilot study. Clin Neurol Neurosurg. 2018;173:124–9.

7. de Sousa MC, Gjorgjieva M, Dolicka D, Sobolewski C, Foti M. Deciphering miRNAs' Action through miRNA Editing. Int J Mol Sci. 2019;20(24):6249.

8. Mohr AM, Mott JL. Overview of microRNA biology. Semin Liver Dis. 2015;35(1):3–11.

9. Supriya M, Christopher R, Indira Devi B, Bhat DI, Shukla D. Circulating microRNAs as potential molecular biomarkers for intracranial aneurysmal rupture. Mol Diagn Ther. 2020;24(3):351–64.

10. Liu D, Han L, Wu X, Yang X, Zhang Q, Jiang F. Genome-wide microRNA changes in human intracranial aneurysms. BMC Neurol. 2014;14:188.

11. Kleinloog R, Verweij BH, van der Vlies P, Deelen P, Swertz MA, de Muynck L, et al. RNA sequencing analysis of intracranial aneurysm walls reveals involvement of lysosomes and immunoglobulins in rupture. Stroke. 2016;47(5):1286–93.

12. Fan W, Liu Y, Li C, Qu X, Zheng G, Zhang Q, et al. microRNA-331-3p maintains the contractile type of vascular smooth muscle cells by regulating TNF-α and CD14 in intracranial aneurysm. Neuropharmacology. 2020;164: 107858.

13. Gao Y, Zhao C, Wang J, Li H, Yang B. The potential biomarkers for the formation and development of intracranial aneurysm. J Clin Neurosci. 2020;81:270–8.

14. Sulsky SI, Fuller WG, Van Landingham C, Ogden MW, Swauger JE, Curtin GM. Evaluating the association between menthol cigarette use and the likelihood of being a former versus current smoker. Regul Toxicol Pharmacol RTP. 2014;70(1):231–41.

15. Frosen J, Cebral J, Robertson AM, Aoki T. Flow-induced, inflammation-mediated arterial wall remodeling in the formation and progression of intracranial aneurysms. Neurosurg Focus. 2019;47(1):E21.

16. He B, Zhao Z, Cai Q, Zhang Y, Zhang P, Shi S, et al. miRNA-based biomarkers, therapies, and resistance in Cancer. Int J Biol Sci. 2020;16(14):2628–47.

17. Molyneux AJ, Kerr RS, Birks J, Ramzi N, Yarnold J, Sneade M, et al. Risk of recurrent subarachnoid haemorrhage, death, or dependence and standardised mortality ratios after clipping or coiling of an intracranial aneurysm in the International Subarachnoid Aneurysm Trial (ISAT): long-term follow-up. Lancet Neurol. 2009;8(5):427–33.

18. Signorelli F, Sela S, Gesualdo L, Chevrel S, Tollet F, Pailler-Mattei C, et al. Hemodynamic stress,

inflammation, and intracranial aneurysm development and rupture: a systematic review. World Neurosurg. 2018;115:234–44.

19. Chu AJ. Antagonism by bioactive polyphenols against inflammation: a systematic view. Inflamm Allergy Drug Targets. 2014;13(1):34–64.

20. Li XG, Wang YB. SRPK1 gene silencing promotes vascular smooth muscle cell proliferation and vascular remodeling via inhibition of the PI3K/Akt signaling pathway in a rat model of intracranial aneurysms. CNS Neurosci Ther. 2019;25(2):233–44.

21. Chen S, Chen H, Yu C, Lu R, Song T, Wang X, et al. Long noncoding RNA myocardial infarction associated transcript promotes the development of thoracic aortic by targeting microRNA-145 via the PI3K/Akt signaling pathway. J Cell Biochem. 2019;120(9):14405–13.

22. Escudero P, Navarro A, Ferrando C, Furio E, Gonzalez-Navarro H, Juez M, et al. Combined treatment with bexarotene and rosuvastatin reduces angiotensin-II-induced abdominal aortic aneurysm in apoE(-/-) mice and angiogenesis. Br J Pharmacol. 2015;172(12):2946–60.

23. Cong X, Kong W. Endothelial tight junctions and their regulatory signaling pathways in vascular homeostasis and disease. Cell Signal. 2020;66: 109485.

24. Hoesel B, Schmid JA. The complexity of NF-κB signaling in inflammation and cancer. Mol Cancer. 2013;12:86.

25. Wang S, Wang Y, Jiang J, Wang R, Li L, Qiu Z, et al. 15-HETE protects rat pulmonary arterial smooth muscle cells from apoptosis via the PI3K/Akt pathway. Prostaglandins Other Lipid Mediat. 2010;91(1–2):51–60.

26. Penn DL, Witte SR, Komotar RJ, Sander Connolly Jr E. The role of vascular remodeling and inflammation in the pathogenesis of intracranial aneurysms. J Clin Neurosci. 2014;21(1):28–32.

27. Yu L, Wang J, Wang S, Zhang D, Zhao Y, Wang R, et al. DNA methylation regulates gene expression in intracranial aneurysms. World Neurosurg. 2017;105:28–36.

28. Kong F, You H, Zheng K, Tang R, Zheng C. The crosstalk between pattern-recognition receptor signaling and calcium signaling. Int J Biol Macromol. 2021;192:745–56.

29. Jayaraman T, Paget A, Shin YS, Li X, Mayer J, Chaudhry H, et al. TNF-alpha-mediated inflammation in cerebral aneurysms: a potential link to growth and rupture. Vasc health Risk Manag. 2008;4(4):805–17.

30. Gerzanich V, Zhang F, West GA, Simard JM. Chronic nicotine alters NO signaling of Ca(2+) channels in cerebral arterioles. Circ Res. 2001;88(3): 359–65.

31. Jin J, Duan J, Du L, Xing W, Peng X, Zhao Q. Inflammation and immune cell abnormalities in intracranial aneurysm subarachnoid hemorrhage (SAH): Relevant signaling pathways and therapeutic strategies. Front Immunol. 2022;13:1027756.

32. Ho AL, Lin N, Frerichs KU, Du R. Smoking and intracranial aneurysm morphology. Neurosurgery. 2015;77(1):59–66 (**discussion**).

33. Lai Z, Lin P, Weng X, Su J, Chen Y, He Y, et al. MicroRNA-574–5p promotes cell growth of vascular smooth muscle cells in the progression of coronary artery disease. Biomed Pharmacother. 2018;97: 162–7.

34. Huang R, Hu Z, Cao Y, Li H, Zhang H, Su W, et al. MiR-652-3p inhibition enhances endothelial repair and reduces atherosclerosis by promoting cyclin D2 expression. EBioMedicine. 2019;40:685–94.

35. Boileau A, Lino Cardenas CL, Courtois A, Zhang L, Rodosthenous RS, Das S, et al. MiR-574–5p: a circulating marker of thoracic aortic aneurysm. Int J Mol Sci. 2019;20(16):3924.

36. Feng X, Qian Z, Zhang B, Guo E, Wang L, Liu P, et al. Number of cigarettes smoked per day, smoking index, and intracranial aneurysm rupture: a case-control study. Front Neurol. 2018;9:380.

37. Boileau A, Lino Cardenas CL, Courtois A, et al. MiR-574-5p: a circulating marker of thoracic aortic aneurysm. Int J Mol Sci. 2019;20(16):3924.

38. Huang W, Zhao Y, Xu Z, Wu X, Qiao M, Zhu Z, et al. The regulatory mechanism of miR-574–5p expression in cancer. Biomolecules. 2022;13(1):40.

39. Zhao M, Xu L, Qian H. Bioinformatics analysis of microRNA profiles and identification of microRNA-mRNA network and biological markers in intracranial aneurysm. Medicine. 2020;99(31): e21186.

40. Nakajima N, Nagahiro S, Sano T, Satomi J, Satoh K. Phenotypic modulation of smooth muscle cells in human cerebral aneurysmal walls. Acta Neuropathol. 2000;100(5):475–80.

41. Shimizu K, Kushamae M, Mizutani T, Aoki T. Intracranial aneurysm as a macrophage-mediated inflammatory disease. Neurol Med Chir (Tokyo). 2019;59(4):126–32.

42. Liu X, Su X, Xu S, Wang H, Han D, Li J, et al. MicroRNA in vivo precipitation identifies miR-151-3p as a computational unpredictable miRNA to target Stat3 and inhibits innate IL-6 production. Cell Mol Immunol. 2018;15(2):99–110.

43. Garbers C, Aparicio-Siegmund S, Rose-John S. The IL-6/gp130/STAT3 signaling axis: recent advances towards specific inhibition. Curr Opin Immunol. 2015;34:75–82.

44. Sugiyama S, Niizuma K, Nakayama T, Shimizu H, Endo H, Inoue T, et al. Relative residence time prolongation in intracranial aneurysms: a possible association with atherosclerosis. Neurosurgery. 2013;73(5):767–76.

45. Ollikainen E, Tulamo R, Lehti S, Lee-Rueckert M, Hernesniemi J, Niemela M, et al. Smooth muscle cell foam cell formation, apolipoproteins, and ABCA1 in intracranial aneurysms: implications for lipid accumulation as a promoter of aneurysm wall rupture. J Neuropathol Exp Neurol. 2016;75(7):689–99.

46. Huang R, Hu Z, Cao Y, et al. MiR-652-3p inhibition enhances endothelial repair and reduces atherosclerosis by promoting Cyclin D2 expression. EBioMedicine. 2019;40:685–94.

47. Chi X, Jiang Y, Chen Y, Lv L, Chen J, Yang F, Zhang X, Pan F, Cai Q. Upregulation of microRNA miR-652-3p is a prognostic risk factor for hepatocellular carcinoma and regulates cell proliferation, migration, and invasion. Bioengineered. 2021;12(1):7519–28.

48. Liu H, Zuo C, Cao L, Yang N, Jiang T. Inhibition of miR-652-3p regulates lipid metabolism and inflammatory cytokine secretion of macrophages to alleviate atherosclerosis by improving TP53 expression. Mediat Inflamm. 2022;2022:9655097.

49. Vegter EL, Ovchinnikova ES, van Veldhuisen DJ, Jaarsma T, Berezikov E, van der Meer P, et al. Low circulating microRNA levels in heart failure patients are associated with atherosclerotic disease and cardiovascular-related rehospitalizations. Clin Res Cardiol. 2017;106(8):598–609.

50. Ostergaard JR. Risk factors in intracranial saccular aneurysms. Aspects on the formation and rupture of aneurysms, and development of cerebral vasospasm. Acta Neurol Scand. 1989;80(2):81–98.

51. Olivieri F, Prattichizzo F, Giuliani A, Matacchione G, Rippo MR, Sabbatinelli J, et al. miR-21 and miR-146a: the microRNAs of inflammaging and age-related diseases. Ageing Res Rev. 2021;70: 101374.